

Aldehyde-Assisted Fractionation Enhances Lignin Valorization in Endocarp Waste Biomass

Jean Behaghel de Bueren, Florent Héroguel, Chloé Wegmann, Graham R. Dick, Raymond Buser, and Jeremy S. Luterbacher*



Cite This: *ACS Sustainable Chem. Eng.* 2020, 8, 16737–16745



Read Online

ACCESS |



Metrics & More



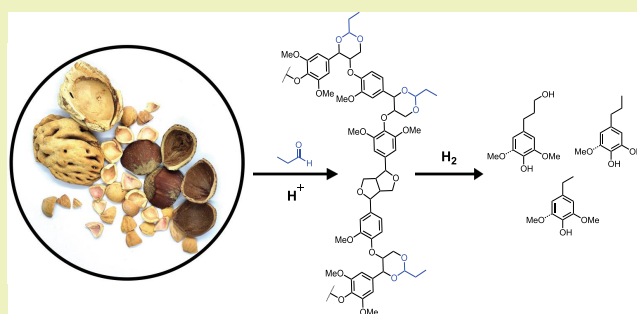
Article Recommendations



Supporting Information

ABSTRACT: Endocarp biomass, which forms much of the inedible portion of nuts and stone fruits, is a promising feedstock for aromatic chemical production due to its high lignin content and because it is a food industry waste. Here, we tested the nut shells and fruit kernels of seven species and report that their aromatic monomer yields can surpass those obtained using wood chips by up to 30% on a dry biomass basis due to their high lignin content. We also observed that acid-catalyzed aldehyde-assisted fractionation (AAF) facilitates lignin valorization when using industrially relevant particle sizes (3–5 mm) with monomers yields that are 80% to 170% higher than those obtained with reductive catalytic fractionation (RCF) for similarly sized particles. This difference was highly correlated with the feedstock surface area, demonstrating the importance of acidic pretreatment for substrates with low accessibility and/or large particles.

KEYWORDS: Lignin, Endocarp biomass, Depolymerization, Food waste, Catalysis, Fractionation, Lignocellulose



INTRODUCTION

Our society relies on fossil resources to produce energy and chemicals. To reduce our dependence on fossil feedstocks and to develop a sustainable chemical industry, renewable carbon feedstocks are needed. Lignocellulosic biomass, which is the main source of renewable carbon on Earth after atmospheric CO₂, will likely play a crucial role in achieving this goal. Lignocellulosic biomass is mainly composed of three biopolymers (cellulose, hemicellulose, and lignin), and isolating each fraction without significant degradation remains a challenge. Specifically, current industrialized fractionation technologies employ acidic, basic, or high temperature conditions that degrade lignin during its isolation through condensation reactions. The most prominent condensation pathway is thought to involve the elimination of benzylic alcohol on the lignin backbone, which produces benzylic carbocation that reacts with neighboring aromatic groups, forming additional carbon–carbon (C–C) bonds.¹ These recalcitrant bonds significantly alter the lignin's ability to be depolymerized selectively. Selective lignin depolymerization involves the cleavage of its ether linkages via reductive,^{2–9} oxidative,^{10–16} or solvolysis¹⁷ pathways as selectively cleaving C–C bonds remains impractical. Condensation increases the fraction of C–C bonds in lignin, thus decreasing the monomers that can be produced from it by ether cleavage.¹⁸

To maximize the production of aromatic monomers, the native β -O-4 ether linkages in lignin can be depolymerized

directly from the native biomass before condensation occurs using reductive catalytic fractionation (RCF, also referred to as direct hydrogenolysis). In this process, native biomass particles are heated in an organic solvent with a heterogeneous metal catalyst in the presence of molecular hydrogen or a hydrogen donating solvent.¹⁹ This process, in the absence of mass transfer limitations and when ensuring close contact between the biomass and catalyst, can lead to a near theoretical yield of aromatic monomers based on full cleavage of ether linkages (between 40 and 55 wt % based on Klason lignin for wild hardwoods and 20%–30% for softwoods).^{3,20–28} The biomass and catalyst can be physically separated by using a cage or in subsequent compartments in a flow reactor, but both systems require rapid transport of lignin intermediates to the catalyst to avoid condensation, which usually necessitates high dilution.^{22–23} As an alternative to preventing condensation by direct conversion, we previously reported a lignin stabilization strategy that involves the use of aldehydes as protecting groups during its isolation, referred to here as aldehyde-assisted fractionation (AAF).^{24–30} The aldehyde reacts with the 1,3-

Received: May 5, 2020

Revised: August 31, 2020

Published: November 2, 2020



Table 1. Compositional Analysis of Biomass Feedstocks

	Moisture (%)	Klason lignin ^a (%)	Cellulose ^{a,c} (%)	Hemicellulose ^{a,d} (%)	Extractives ^a (%)	Ashes ^a (%)
Birch	6.1	19.1 ^b	34.2 ^b	22.0 ^b	3.5 ^b	0.2
Beech	6.5	21.4 ^b	35.5 ^b	20.9 ^b	3.3 ^b	0.2
Pine	6.0	33.5	ND	ND	6.0	0.3
Cedar	9.0	31.5	ND	ND	2.7	0.4
Plum kernel	7.0	36.7	22.1	24.2	3.7	0.3
Apricot kernel	6.1	36.0	19.9	27.4	10.0	0.3
Peach kernel	5.9	36.8	20.3	25.4	10.4	0.4
Cherry kernel	4.7	37.6	20.1	25.5	14.1	0.4
Hazelnut shell	7.5	41.3	18.7	23.1	5.5	1.0
Walnut shell	5.4	43.9	13.4	10.4	20.4	3.6
Almond shell	8.9	31.6	23.6	27.6	5.1	0.7

^aFractions are presented as a weight percentage of the biomass on a dry basis. ^bData from Talebi Amiri et al.³⁰ ^cBased on the glucan fraction.

^dBased on the xylan, galactan, arabinan, and mannan fractions.

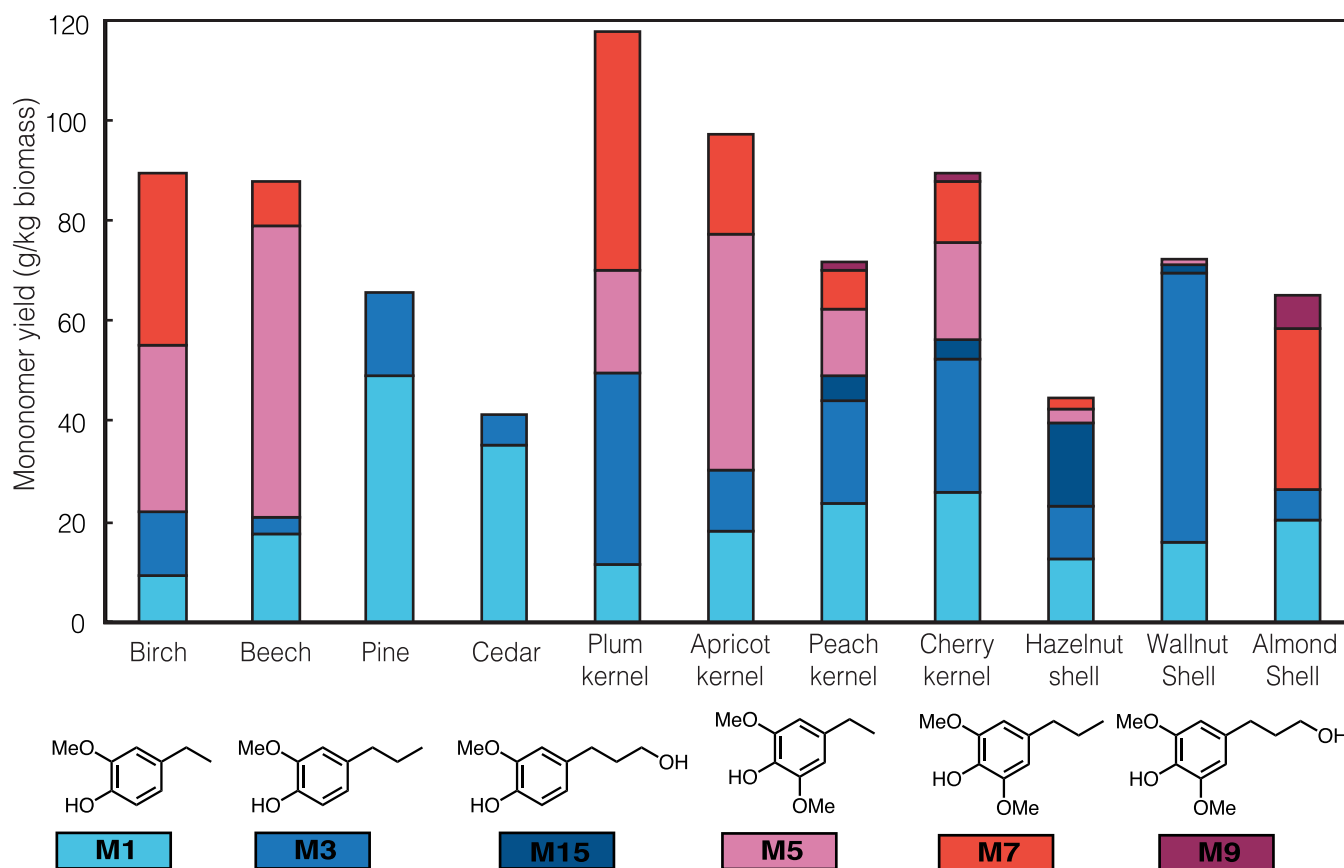


Figure 1. Biomass feedstocks RCF (reaction conditions: 250 °C, 40 bar H₂, 15 h; solvent: THF; catalyst: Ru/C; biomass particle size: 50–125 μm). Guaiacyl (G) and syringyl monomers (S) are given in shades of blue and red, respectively. Yields are expressed on a dry biomass basis.

diol of the native β -O-4 structure to form an acetal that prevents benzylic alcohol elimination, which is the first step in the condensation pathway. Acetal protection also allows the biomass to be fractionated and lignin to be isolated from the other biomass fractions, while retaining the majority of its ether linkages. After subsequent depolymerization of the stabilized lignin by hydrogenolysis, observed yields were usually within 5%–10% of those obtained by RCF using wood as a benchmark to evaluate the quality of the stabilization and isolation process.³⁰ Besides reductive chemistry and acetal stabilization, other strategies were developed to efficiently convert lignin into monomers by avoiding condensation. Among these, oxidative catalytic

fractionation under alkaline conditions^{31,32} and photocatalysis under mild conditions³³ were reported as efficient methods to reach high yields of monophenolic compounds from native lignin in biomass.

Though most studies have focused on wood, a particularly interesting source of nonedible lignocellulosic biomass are endocarps. In stone fruits, the endocarp is the thick hard layer that surrounds the seed in the pit. In nuts, it is the hard layer that surrounds the edible kernel. Unlike most nonedible crop residues, endocarp biomass cannot be used for livestock feed and is largely underutilized.³⁴ In addition to its availability within the food production logistics chain, its high lignin content (up to 50 wt %)³⁵ gives it a high energy density and

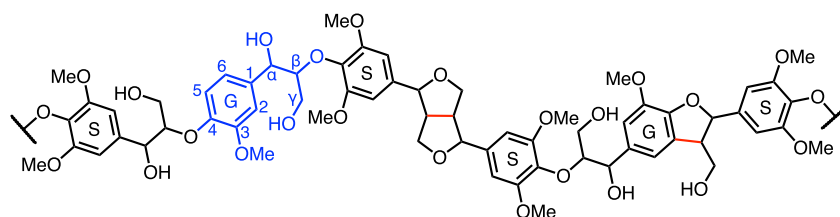


Figure 2. Lignin model structure for hardwood.³⁹ The structure of one β -O-4 linkage is highlighted in blue. Recalcitrant native C–C linkages are highlighted in red. G: guaiacyl; S: syringyl.

makes it an attractive source of aromatics.³⁵ While its potential for energy production has already been explored,³⁴ the biorefining of this waste into chemicals has seen limited studies.³⁵ Here, we explore the depolymerization of various endocarp lignin streams by using both RCF and AAF and demonstrate that endocarp biomass offers unique opportunities for aromatic monomer production. We also demonstrate that atypical physical characteristics such as low surface area and varying chemical functionality within the native lignin have substantial effects on the aromatic monomer yields resulting from different lignin upgrading methods.

RESULTS AND DISCUSSION

Compositional Analysis of Raw Feedstocks. To comprehensively study the depolymerization of different endocarps and compare them to classic biomass valorization feedstocks, we selected 12 materials from various biomass species including hardwood chips, softwood chips, fruit kernels, and nut shells (Table 1). Each feedstock was sieved after grinding and ball milling to obtain three particle size fractions: 50–125 μm , 0.5–1.0 mm, and 3–5 mm. These fractions were separately subjected to RCF and AAF, and the resulting yields of aromatic monomers were compared to exclude any effect that sieving might have had on the fractions' compositions and thus the conclusions of this work. Compositional analyses were performed on fractions with the smallest particles and revealed high lignin contents for endocarps as compared to woods (Table 1), with a maximum Klason lignin content of 43.9 wt % for walnut shells. As some have noted, the determination of Klason lignin content in unusual biomass material such as seed coats and food wastes can be prone to overestimation, and thus, these numbers should be considered as estimates rather than exact quantities.^{36,37} However, as we discuss, these high lignin contents are largely confirmed by the associated high monomer yields that can be obtained from these feedstocks (*vide infra*). An additional chloroform extraction has been reported to remove additional extractives that can interfere with Klason lignin quantification in seeds (see SI Section S3.6.1).³⁶ We performed this procedure as an additional control, but the Klason lignin contents obtained after such treatment differ only slightly from those obtained with an already reported procedure (Table S7).³⁰ The endocarp feedstocks studied here also had a lower cellulose contents and higher hemicellulose contents than softwoods and hardwoods. The sole exception was walnut shells, which contained less hemicellulose. These results are consistent with previously reported compositional analyses of endocarps.³⁸

Potential Monomer Production on Endocarp Feedstocks. Because RCF typically produces near theoretical yields of aromatic monomers through ether cleavage, we performed RCF (THF, Ru/C, 250 $^{\circ}\text{C}$, 40 bar H_2 , 15h) on all selected feedstocks to compare the maximum quantity of achievable

monomer yields for each species (Figure 1). Tetrahydrofuran (THF) was chosen as the solvent and Ru/C as the catalyst to match previous studies on the depolymerization of extracted lignin.³⁰ The results obtained when using THF as the solvent for RCF of wood are within a few percentage points of those obtained when methanol was used ($\geq 95\%$, Figure S1).^{2,3,6} Only the product distribution is affected, notably due to an increase in the fraction of chain truncation products. Greater differences could be observed when larger particles of endocarp biomass were used (70% for apricot pits 3–5 mm, Figure S1), but the differences were not significant compared to the various trends discussed in the study. To avoid any accessibility issues or mass transfer limitations, we used the smallest particle size fraction (50–125 μm), and the resulting monomers yields were within the range of previously reported results with respect to Klason lignin content (Table S1). For example, RCF of birch and beech woods gave monomer yields of 47 and 41 wt % with respect to Klason lignin, respectively. These are within the range expected for the maximum yield of hardwoods (40%–55%).^{3,20–28,24–26} Detailed yield calculations are described in SI Section S2.6.

Hardwoods (birch, beech) and softwoods (pine, cedar) were used as references since they are well studied in the literature. They have different lignin structures (Figure 2) and differing abundancies of guaiacyl (G) and syringyl (S) residues. We characterized the abundance using the proportion of guaiacyl units and defined it as $G/(G+S)$, which was computed using the hydrogenolysis monomer distribution. Although this method only provides an indirect indicator of the composition of native lignin, the ratio calculated based on hydrogenolysis monomer distribution closely tracks the $G/(G+S)$ ratio that was calculated by peak integration of the ^1H – ^{13}C heteronuclear single quantum coherence nuclear magnetic resonance (HSQC-NMR) spectrum of isolated lignin (Table S1). For apricot kernel lignin, the same $G/(G+S)$ ratio (47%) was found by using the hydrogenolysis product distribution and the HSQC-NMR peaks integration. For almond shell lignin, 37% and 40% were found via product distribution and HSQC-NMR, respectively. Deviations of 9%, 10%, and 13% were observed, respectively, for birch, hazelnut shell, and plum shell lignins.

Hardwood lignins mostly contain syringyl units ($G/(G+S)$ are 24% for both birch and beech (Table S1)), while softwood lignins are known to contain only guaiacyl units ($G/(G+S)$ are 100% (Table S1)). Softwood lignins have also been reported to have more native C–C bonds in their structure.¹ This phenomenon has been proposed to be due to their pure guaiacyl content as guaiacyl species have one less aromatic methoxy group than syringyl species (position 5, Figure 2). These positions can form recalcitrant C–C bonds during lignin biosynthesis,¹ lowering theoretical monomer yields based on ether cleavage. Nevertheless, softwoods offer valorization

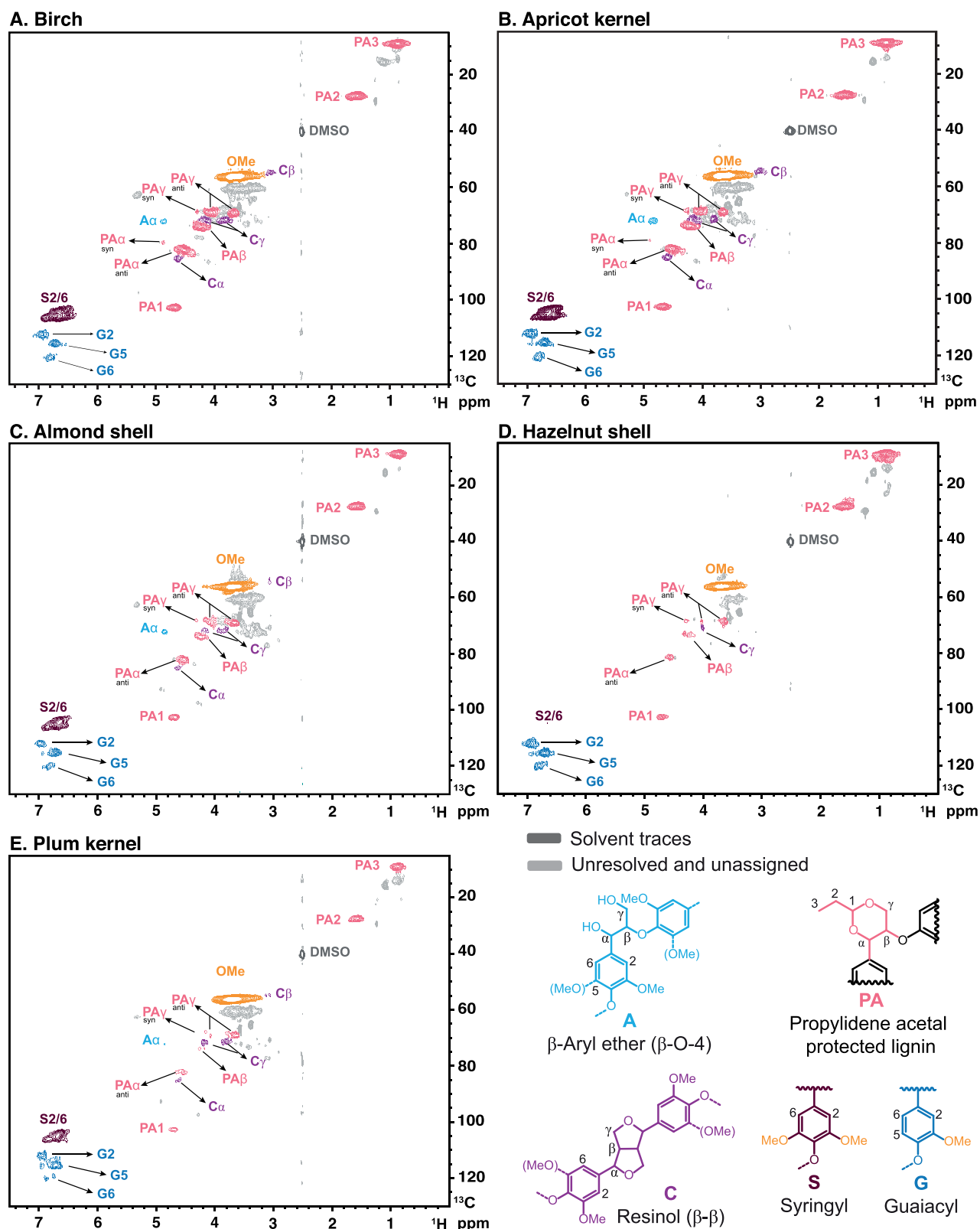


Figure 3. HSQC-NMR spectra of isolated lignin extracted using AAF with propionaldehyde (3 h, 85 °C, particle size 50–125 μ m).

opportunities related to guaiacyl-derived molecules such as vanillin or eugenol that have large existing commercial markets unlike their syringyl equivalents.

All the endocarp biomass feedstocks considered here led to monomer yields per total biomass within the same order of magnitude as the wood references. Cherry, apricot, and plum

pits surpassed birch yields (89.5 g monomers/kg dry biomass) with yields of 89.6, 97.2, and 117.7 g/kg, respectively. We observed a wide variability in G and S monomer distributions with G/(G+S) ratios ranging from 99% for walnut shells to 31% for apricot pits (Table S1). These differences offer the possibility of tuning the selectivity between G and S monomers

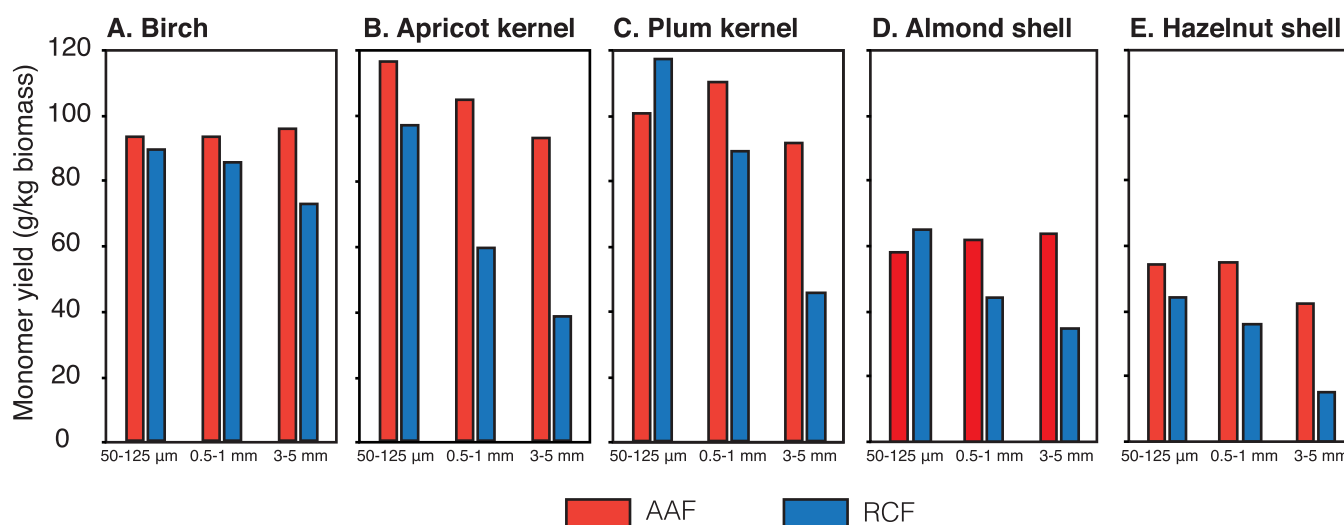


Figure 4. Lignin-derived monomer yields obtained by RCF and AAF followed by hydrogenolysis of the extracted lignin for selected biomass species using three separate particle size ranges as a starting material. Yields are expressed on a dry biomass basis. RCF conditions: THF, Ru/C, 250 °C, 15 h, 40 bar H₂. AAF conditions: lignin extraction with dioxane, propionaldehyde, HCl at 3 h for 85 °C followed by isolated lignin hydrogenolysis (THF, Ru/C, 250 °C, 3 h, 40 bar H₂).

through feed selection. HSQC-NMR spectra of the isolated lignin with AAF (Figure 3) show clear compositional differences between feedstocks in the aromatic region (¹H: 6.4–7.2 ppm; ¹³C: 100–125 ppm), which is in agreement with the wide monomer distributions measured after depolymerization. The peaks assigned to propylidene acetal-protected lignin structures were greater than those assigned for free β-O-4 ether linkages confirming efficient lignin stabilization during AAF on endocarp biomass (Figure 3). Specifically, the comparison of a peak assigned to the propylidene acetal structure (PA1, Figure 3) and a peak related to the free β-O-4 ether linkage (Aα, Figure 3) allowed us to estimate the degree of protection of β-O-4 structures. All the extracted lignins showed high degrees of protection (89%, 80%, 75%, 100%, and 64% for birch, apricot kernels, almonds shells, hazelnut shells, and plum kernels, respectively).

More generally, this screening highlights the high aromatic production potential of endocarp biomass, which is typically available at lower price than wood due to waste management costs and typically do not require further drying or size reduction.

Effect of Particle Size on RCF and AAF Efficiency. RCF studies are usually conducted on biomass thoroughly milled into sawdust,^{3,21} which tends to suppress any accessibility limitations. However, in an industrial context, biomass chips (>1 cm) are likely to be used because size reduction steps are costly and energy intensive, especially considering the hardness of endocarp feedstocks. Size reduction simultaneously increases the specific area of the biomass and also decreases delignification mass transfer limitations thanks to shorter diffusion lengths. The effects of these two phenomena occur in concert and, as such, are very challenging to dissociate. We therefore consider that both effects are encompassed by the term accessibility in this work.

To verify the effect of size reduction, we used AAF to isolate lignin from five selected feedstocks with three different particle size ranges and then hydrogenolyzed those lignins and compared the results to those obtained by using RCF (Figure 4). Starting with birch, RCF yields dropped slightly with increasing particle size, obtaining yields of 89.5, 85.8, and 72.9

g/kg for wood particle fractions of 50–125 μm, 0.5–1 mm, and 3–5 mm, respectively (Figure 4A). Conversely, hydrogenolysis of lignin isolated via AAF was not affected by particle size, and we even observed a slight increase (2.7%) as the size of the particles increased, which we assigned to experimental variability.

The reduction in monomer yield trends for RCF as a function of particle size was more pronounced for other types of biomass. When switching from small (50–125 μm) to large (3–5 mm) fruit pit particles, RCF yields decreased by more than 60% (Figure 4B, C). The greater bulk density of these biomass species likely decreased lignin accessibility, emphasizing the importance of size reduction. We observed the same decreases for nut shells with hazelnut shells yielding 65% less and almond shells yielding 47% less (Figure 4D, E). The improved yield reduction observed for almond shells could be attributed to their higher accessibility as compared to the other endocarp biomass feedstocks (*vide infra*, Figure 6).

When performing AAF and isolating the stabilized lignin prior to its hydrogenolysis, yield reductions were significantly less pronounced for endocarps as a function of increasing particle size (Figure 4A–E). With the largest particle size, yields using apricots and plum pits were reduced by 8% and 20%, respectively, a decrease 3-fold smaller than that observed for RCF. With almonds, yields obtained by AAF increased by 5% and 10% when switching from small to medium and small to large particles, respectively. When using hazelnut shells, monomer yields decreased by 22% when switching from small to large particles, while small- and medium-sized particles produced similar yields (<1% difference). In all cases, RCF saw the greatest reduction in monomer yields as a function of increasing particle size.

When using AAF on plum kernels, almond shells, and hazelnut shells, the best yield was not observed when the smallest particles were used, consistent with our observation with birch wood (Figure 4). This result indicates that the pretreatment protocol likely requires optimization for each particle size. The standard procedure³⁰ (3 h) was optimized for wood sawdust (0.45–6 mm), but residence times should be tuned to each biomass sample, according to its nature and

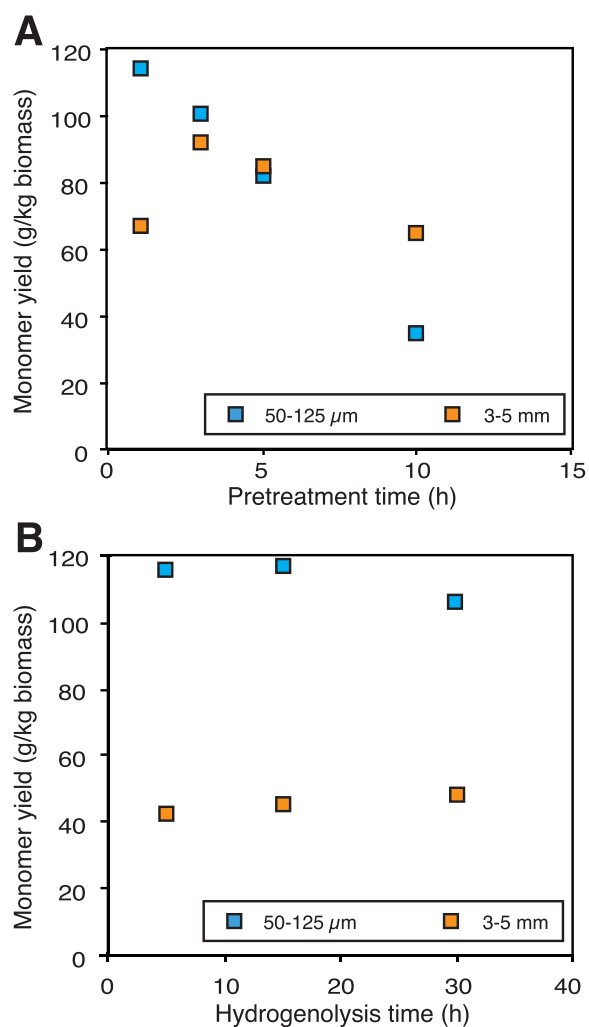


Figure 5. Evolution of monomer yields for large and small plum pit particles. Yields are expressed on a dry biomass basis. (A) Pretreatment and lignin extraction was performed using different residence times at 80 °C, while identical hydrogenolysis conditions were used (THF, Ru/C, 250 °C, 40 bar H₂, 3 h). (B) RCF was performed directly on native biomass (THF, Ru/C, 250 °C, 40 bar H₂) at different residence times.

particle size. We varied the pretreatment time between 1 and 10 h for large and small plum pit particles to evaluate its effect on the extracted lignin's hydrogenolysis yields (Figure 5A). For the small particles, the best monomer yields were obtained after only 1 h and decreased with additional residence time. Most of the lignin was likely extracted after 1 h, following which, due to the reversible nature of the acetal protection, the lignin likely gradually condensed. For the largest particles, the maximum yield after hydrogenolysis was obtained after a 3 h pretreatment. As previously demonstrated for similar systems, longer pretreatment times were likely required to deconstruct the lignocellulose structure and fully extract the lignin.^{25,30} Extending the pretreatment time beyond 3 h reduced monomer yields, as once the lignin is extracted, condensation is thermodynamically preferred. Increasing biomass residence time in a pretreatment reactor is likely to require additional energy. Future studies could compare this energy demand with size reduction requirements during biomass preparation.

One explanation for the reduction in aromatic monomer yields as a function of increasing particle size for RCF could be

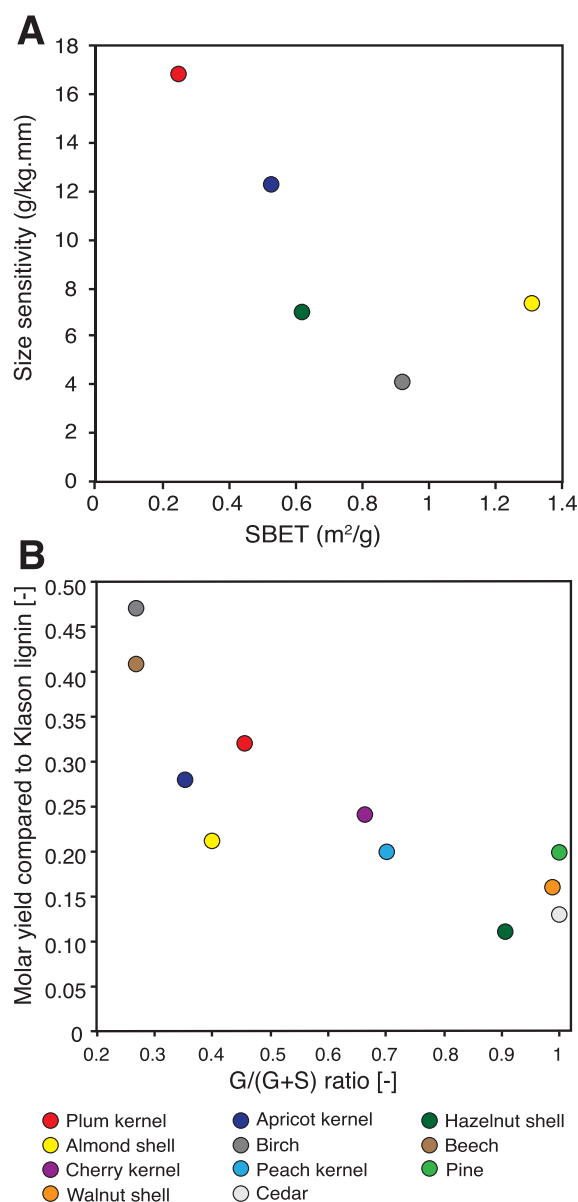


Figure 6. Influence of porosity and S/(G+S) ratio on RCF lignin monomer yields. Yields are expressed on a dry biomass basis. (A) Monomer yield sensitivity to biomass particle size for RCF as a function of Brunauer–Emmett–Teller surface (SBET). The size sensitivity is expressed as the decrease in aromatic monomer yield per mm change of biomass particle size (g/(kg biomass mm particle size)). (B) Aromatic monomer yield on a Klason lignin basis obtained by RCF for different feedstocks (50–125 μm) as a function of the G(S+G) ratio in the product mixture (reaction condition: THF, Ru/C, 250 °C, 15 h, 40 bar H₂).

that longer residence times were required to fully extract the lignin. Therefore, we also investigated the dependence of monomer yield on RCF residence time using plum pits. For both large and small particles, monomer yields were not time sensitive with observed yield variations under 15% between 5 and 30 h (Figure 5B).³⁹ These observations confirmed previous reports that the phenolic monomers are stable under hydrogenolysis conditions³ further supporting our hypothesis that yields are limited by lignin accessibility. As lignin needs to be solubilized in order to be hydrogenolyzed,

increased degradation of lignin fragments by condensation will be observed as the necessary diffusion distance grows.

Overall, yields obtained from the hydrogenolysis of isolated lignin resulting from a pretreatment and stabilization stage were significantly less sensitive to initial particle size than those obtained from directly subjecting native biomass to hydrogenolysis. Fractionation increased lignin accessibility during hydrogenolysis and largely negated any effects of the original particle size. Also, as the protection group is a soluble aldehyde, it could diffuse within the biomass's pore network and stabilize the lignin before the biomass is deconstructed. In the RCF system, the stabilizing agent is the metal catalyst which is supported on particles that are too big to enter biomass pores.⁴⁰ As the diffusion length through the catalyst and biomass increases with biomass particle size, reactive lignin intermediates are more likely to undergo partial condensation before contacting the stabilizing catalyst. In comparison, AAF lignin is assumed to be less sensitive to diffusion length as it is presumably stabilized somewhat independently of biomass particle size due to the capacity of the aldehyde to penetrate the biomass. Of course, for hydrogenolysis, both stabilized AAF lignin and reactive RCF intermediates need to diffuse through the catalyst to the Ru surface. Since AAF lignin is assumed to be very similar to RCF lignin after the initial solvolysis and since the same catalyst was used in both cases, diffusion through the catalyst is assumed to be similar. Even if there is a difference, because the lignin fragments resulting from AAF are stabilized, they are likely to be fairly insensitive to this diffusion as well. Importantly, the distribution of monomers was never significantly affected by the depolymerization method or the particle size (Table S2).

Influence of Porosity and G/(S+G) Ratio on Monomer yield. To rationalize yield variations, we investigated the influence of porosity as an indicator of lignin accessibility. Prior to porosity measurements, extractives were removed by washing the material with water–ethanol mixtures. The subsequent drying was carefully performed as it is known to lead to pore collapse.⁴¹ To limit the effect of structural changes during drying, specifically through pore collapse, we performed critical point drying (CPD) on all samples by supercritical CO₂ (see details in SI Section S2.6). To illustrate the importance of careful drying, we observed a 3-fold reduction in surface area when switching from CPD to vacuum drying for native birch samples (Table S3, entries 1 and 2). Porosity measurements suggested that the higher accessibility of birch, which had a porous volume twice that of apricots pits and hazelnut shells, could explain why RCF monomer yields did not drop as much for hardwoods compared to endocarps as particle size increased. A higher accessibility would likely lead to faster transport between the biomass's inner structure and the catalyst's surface. Ball milling likely decreased the length of the diffusion path but also increased specific surface area. For hazelnut shells, we saw a 3-fold increase in surface area and porous volume after ball milling (Table S3, entries 6 and 7), which correlates strongly with the 3-fold increase in monomer yield obtained by RCF (Figure 4E). Interestingly, almond shells which had a higher porosity than other endocarp biomass samples showed the lowest yield sensitivity to particle size when using RCF. Although not perfectly linear, there is a clear trend between yield sensitivity to particle size for RCF and the measured biomass porosity (Figure 6A), suggesting that particle size and accessibility could be one of the important factors playing a role in controlling RCF yields.

Thus, processes that employ a pretreatment step might be better suited to treating larger particles, especially for low-accessibility substrates. However, both economic and sustainability factors would need to be considered before any definitive assessment, which is beyond the scope of this study.

As endocarp biomass covers a large range of G/(S+G) ratios, which we measure indirectly through our product distribution, we explored the relationship between this ratio and the depolymerization yields on a Klason lignin basis (Figure 6B). A higher guaiacyl content in the lignin consistently led to a lower molar depolymerization yields. In past work, it was argued that this resulted from increased formation of recalcitrant C–C bonds during lignin biosynthesis stemming from the reduced aromatic methoxylation of guaiacyl subunits as compared to syringyl subunits.¹ Nevertheless, a recent study⁴² showed that additional factors beyond monomeric composition influence monomer yields, such as monomer transport during lignin synthesis in the plant, and therefore, the correlation we observe here may be a proxy for another causal effect, especially considering the uncertainty in Klason lignin measurements for endocarps. A comparison of the results plotted with respect Klason lignin contents obtained with and without a chloroform extraction is also provided in the Figure S3, but both show the same trends.

CONCLUSION

We have demonstrated the significant potential of endocarp biomass feedstocks for renewable aromatic production due to their high lignin content compared to wood. While near-maximum yields can be achieved with RCF when using ball-milled feedstocks, the low lignin accessibility in shells and kernels prevents efficient extraction when using larger particles. Due to acid-mediated biomass deconstruction and efficient diffusion of the protecting agent into the inner biomass structure, hydrogenolysis yields obtained with AAF-isolated lignin were much less particle size sensitive. As a result, near maximum yields could be obtained with industry-relevant particles sizes. In light of these results, endocarp biomass deconstructed with AAF could constitute an attractive biorefinery scheme, especially considering the low price, low water content, and availability of this feedstock.

ASSOCIATED CONTENT

Supporting Information

The Supporting Information is available free of charge at <https://pubs.acs.org/doi/10.1021/acssuschemeng.0c03360>.

Yield and porosity data, sensitivity analysis to catalyst loading for RCF, influence of chloroform extraction on klason lignin measurement, solvent comparison for the RCF of biomass, detailed experimental procedures for RCF and AAF and isolated lignin hydrogenolysis, chemicals and materials, yield calculation methods, and biomass characterization procedures (PDF)

AUTHOR INFORMATION

Corresponding Author

Jeremy S. Luterbacher – *Laboratory of Sustainable and Catalytic Processing, Institute of Chemical Sciences and Engineering, École Polytechnique Fédérale de Lausanne (EPFL), 1025 Lausanne, Switzerland*; orcid.org/0000-0002-0967-0583; Email: jeremy.luterbacher@epfl.ch

Authors

Jean Behaghel de Bueren – Laboratory of Sustainable and Catalytic Processing, Institute of Chemical Sciences and Engineering, École Polytechnique Fédérale de Lausanne (EPFL), 1025 Lausanne, Switzerland

Florent Héroguel – Laboratory of Sustainable and Catalytic Processing, Institute of Chemical Sciences and Engineering, École Polytechnique Fédérale de Lausanne (EPFL), 1025 Lausanne, Switzerland; orcid.org/0000-0003-2210-7119

Chloé Wegmann – Laboratory of Sustainable and Catalytic Processing, Institute of Chemical Sciences and Engineering, École Polytechnique Fédérale de Lausanne (EPFL), 1025 Lausanne, Switzerland

Graham R. Dick – Laboratory of Sustainable and Catalytic Processing, Institute of Chemical Sciences and Engineering, École Polytechnique Fédérale de Lausanne (EPFL), 1025 Lausanne, Switzerland; orcid.org/0000-0001-5544-6868

Raymond Buser – Laboratory of Sustainable and Catalytic Processing, Institute of Chemical Sciences and Engineering, École Polytechnique Fédérale de Lausanne (EPFL), 1025 Lausanne, Switzerland

Complete contact information is available at:

<https://pubs.acs.org/10.1021/acssuschemeng.0c03360>

Notes

The authors declare the following competing financial interest(s): J.B.B., F.H., C.W., R.B., and J.S.L. are part owners in Bloom Biorenewables Ltd., which is exploring commercial opportunities for aldehyde-assisted fractionation (AAF).

ACKNOWLEDGMENTS

This work was supported by the Swiss National Science Foundation (SNSF) through the SNSF Assistant Professor Energy Grant PYAPP215428, Gebert Rüf Stiftung grant GRS-082/17, Innosuisse Grant 27945.1 PFIW-IW, and EPFL Playgrant PLAY 18-01 Bloom. This work was also supported by the Cooperation and Development Center (Codev) of EPFL through a Development Impact (DI) grant. We thank Valentin Perillat for preliminary work and Aurelien Bornet for assistance with NMR measurements. We are thankful to Barry Callebaut for providing almond and hazelnut shells; Kerntec for providing peach, plum, cherry, and apricot pits, le moulin de Severy for providing walnut shells; Michael Studer for providing birch and beech, and Patrick Arnold for providing pine and cedar.

REFERENCES

- (1) Shuai, L.; Talebi Amiri, M.; Luterbacher, J. S. The Influence of Interunit Carbon-Carbon Linkages during Lignin Upgrading. *Curr. Opin. Green Sustain. Chem.* **2016**, *2*, 59–63.
- (2) Liao, Y.; Koelewijn, S.-F.; Van den Bossche, G.; Van Aelst, J.; Van den Bosch, S.; Renders, T.; Navare, K.; Nicolai, T.; Van Aelst, K.; Maesen, D.; Matsushima, H.; Thevelein, J.; Van Acker, K.; Lagrain, B.; Verboeckend, D.; Sels, B. F. A Sustainable Wood Biorefinery for Low-Carbon Footprint Chemicals Production. *Science* **2020**, *367*, No. 1385.
- (3) Van den Bosch, S.; Schutyser, W.; Vanholme, R.; Driessen, T.; Koelewijn, S.-F.; Renders, T.; De Meester, B.; Huijgen, W. J. J.; Dehaen, W.; Courtin, C. M.; Lagrain, B.; Boerjan, W.; Sels, B. F. Reductive Lignocellulose Fractionation into Soluble Lignin-Derived Phenolic Monomers and Dimers and Processable Carbohydrate Pulp. *Energy Environ. Sci.* **2015**, *8* (6), 1748–1763.
- (4) Galkin, M. V.; Sawadjoon, S.; Rohde, V.; Dawange, M.; Samec, J. S. M. Mild Heterogeneous Palladium-Catalyzed Cleavage of β -O

–4'-Ether Linkages of Lignin Model Compounds and Native Lignin in Air. *ChemCatChem* **2014**, *6* (1), 179–184.

- (5) Shao, Y.; Xia, Q.; Dong, L.; Liu, X.; Han, X.; Parker, S. F.; Cheng, Y.; Daemen, L. L.; Ramirez-Cuesta, A. J.; Yang, S.; Wang, Y. Selective Production of Arenes via Direct Lignin Upgrading over a Niobium-Based Catalyst. *Nat. Commun.* **2017**, *8* (1), na DOI: [10.1038/ncomms16104](https://doi.org/10.1038/ncomms16104).

- (6) Renders, T.; Van den Bossche, G.; Vangeel, T.; Van Aelst, K.; Sels, B. Reductive Catalytic Fractionation: State of the Art of the Lignin-First Biorefinery. *Curr. Opin. Biotechnol.* **2019**, *56*, 193–201.

- (7) Anderson, E. M.; Stone, M. L.; Hülsey, M. J.; Beckham, G. T.; Román-Leshkov, Y. Kinetic Studies of Lignin Solvolysis and Reduction by Reductive Catalytic Fractionation Decoupled in Flow-Through Reactors. *ACS Sustainable Chem. Eng.* **2018**, *6* (6), 7951–7959.

- (8) Cheng, C.; Truong, J.; Barrett, J. A.; Shen, D.; Abu-Omar, M. M.; Ford, P. C. Hydrogenolysis of Organosolv Lignin in Ethanol/Isopropanol Media without Added Transition-Metal Catalyst. *ACS Sustainable Chem. Eng.* **2020**, *8* (2), 1023–1030.

- (9) Van den Bosch, S.; Schutyser, W.; Koelewijn, S.-F.; Renders, T.; Courtin, C. M.; Sels, B. F. Tuning the Lignin Oil OH-Content with Ru and Pd Catalysts during Lignin Hydrogenolysis on Birch Wood. *Chem. Commun.* **2015**, *51* (67), 13158–13161.

- (10) Vangeel, T.; Schutyser, W.; Renders, T.; Sels, B. F. Perspective on Lignin Oxidation: Advances, Challenges, and Future Directions. *Top. Curr. Chem.* **2018**, *376* (4), na DOI: [10.1007/s41061-018-0207-2](https://doi.org/10.1007/s41061-018-0207-2).

- (11) Lan, W.; de Bueren, J. B.; Luterbacher, J. S. Highly Selective Oxidation and Depolymerization of α,γ -Diol-Protected Lignin. *Angew. Chem., Int. Ed.* **2019**, *58* (9), 2649–2654.

- (12) Rahimi, A.; Ulbrich, A.; Coon, J. J.; Stahl, S. S. Formic-Acid-Induced Depolymerization of Oxidized Lignin to Aromatics. *Nature* **2014**, *515* (7526), 249–252.

- (13) Rahimi, A.; Azarpira, A.; Kim, H.; Ralph, J.; Stahl, S. S. Chemoselective Metal-Free Aerobic Alcohol Oxidation in Lignin. *J. Am. Chem. Soc.* **2013**, *135* (17), 6415–6418.

- (14) Salonen, H. E. P.; Mecke, C. P. A.; Karjomaa, M. I.; Joensuu, P. M.; Koskinen, A. M. P. Copper Catalyzed Alcohol Oxidation and Cleavage of β -O-4 Lignin Model Systems: From Development to Mechanistic Examination. *Chemistry Select* **2018**, *3* (44), 12446–12454.

- (15) Lancefield, C. S.; Ojo, O. S.; Tran, F.; Westwood, N. J. Isolation of Functionalized Phenolic Monomers through Selective Oxidation and C-O Bond Cleavage of the β -O-4 Linkages in Lignin. *Angew. Chem., Int. Ed.* **2015**, *54* (1), 258–262.

- (16) Zhang, C.; Li, H.; Lu, J.; Zhang, X.; MacArthur, K. E.; Heggen, M.; Wang, F. Promoting Lignin Depolymerization and Restraining the Condensation via an Oxidation-Hydrogenation Strategy. *ACS Catal.* **2017**, *7* (5), 3419–3429.

- (17) Kumanaiev, I.; Subbotina, E.; Sävmarker, J.; Larhed, M.; Galkin, M. V.; Samec, J. S. M. Lignin Depolymerization to Monophenolic Compounds in a Flow-through System. *Green Chem.* **2017**, *19* (24), 5767–5771.

- (18) Questell-Santiago, Y. M.; Galkin, M. V.; Barta, K.; Luterbacher, J. S. Stabilization Strategies in Biomass Depolymerization Using Chemical Functionalization. *Nat. Rev. Chem.* **2020**, *4*, 311–330.

- (19) Ferrini, P.; Rinaldi, R. Catalytic Biorefining of Plant Biomass to Non-Pyrolytic Lignin Bio-Oil and Carbohydrates through Hydrogen Transfer Reactions. *Angew. Chem., Int. Ed.* **2014**, *53* (33), 8634–8639.

- (20) Parsell, T.; Yohe, S.; Degenstein, J.; Jarrell, T.; Klein, I.; Gencer, E.; Hewetson, B.; Hurt, M.; Kim, J. I.; Choudhari, H.; Saha, B.; Meilan, R.; Mosier, N.; Ribeiro, F.; Delgass, W. N.; Chapple, C.; Kenttämaa, H. I.; Agrawal, R.; Abu-Omar, M. M. A Synergistic Biorefinery Based on Catalytic Conversion of Lignin Prior to Cellulose Starting from Lignocellulosic Biomass. *Green Chem.* **2015**, *17* (3), 1492–1499.

- (21) Galkin, M. V.; Samec, J. S. M. Selective Route to 2-Propenyl Aryls Directly from Wood by a Tandem Organosolv and Palladium-

Catalysed Transfer Hydrogenolysis. *ChemSusChem* **2014**, *7* (8), 2154–2158.

(22) Lai, C.; Tu, M.; Xia, C.; Shi, Z.; Sun, S.; Yong, Q.; Yu, S. Lignin Alkylation Enhances Enzymatic Hydrolysis of Lignocellulosic Biomass. *Energy Fuels* **2017**, *31* (11), 12317–12326.

(23) Yan, N.; Zhao, C.; Dyson, P. J.; Wang, C.; Liu, L.; Kou, Y. Selective Degradation of Wood Lignin over Noble-Metal Catalysts in a Two-Step Process. *ChemSusChem* **2008**, *1* (7), 626–629.

(24) Van den Bosch, S.; Renders, T.; Kennis, S.; Koelewijn, S.-F.; Van den Bossche, G.; Vangeel, T.; Deneyer, A.; Depuydt, D.; Courtin, C. M.; Thevelein, J. M.; Schutyser, W.; Sels, B. F. Integrating Lignin Valorization and Bio-Ethanol Production: On the Role of Ni-Al₂O₃ Catalyst Pellets during Lignin-First Fractionation. *Green Chem.* **2017**, *19* (14), 3313–3326.

(25) Luo, H.; Klein, I. M.; Jiang, Y.; Zhu, H.; Liu, B.; Kenttämaa, H. I.; Abu-Omar, M. M. Total Utilization of Miscanthus Biomass, Lignin and Carbohydrates, Using Earth Abundant Nickel Catalyst. *ACS Sustainable Chem. Eng.* **2016**, *4* (4), 2316–2322.

(26) Anderson, E. M.; Stone, M. L.; Katahira, R.; Reed, M.; Beckham, G. T.; Román-Leshkov, Y. Flowthrough Reductive Catalytic Fractionation of Biomass. *Joule* **2017**, *1* (3), 613–622.

(27) Lan, W.; Luterbacher, J. S. Preventing Lignin Condensation to Facilitate Aromatic Monomer Production. *Chimia* **2019**, *73* (7), 591–598.

(28) Shuai, L.; Amiri, M. T.; Questell-Santiago, Y. M.; Héroguel, F.; Li, Y.; Kim, H.; Meilan, R.; Chapple, C.; Ralph, J.; Luterbacher, J. S. Formaldehyde Stabilization Facilitates Lignin Monomer Production during Biomass Depolymerization. *Science* **2016**, *354* (6310), 329–333.

(29) Lan, W.; Amiri, M. T.; Hunston, C. M.; Luterbacher, J. S. Protection Group Effects During α,γ -Diol Lignin Stabilization Promote High-Selectivity Monomer Production. *Angew. Chem.* **2018**, *130* (5), 1370–1374.

(30) Talebi Amiri, M.; Dick, G. R.; Questell-Santiago, Y. M.; Luterbacher, J. S. Fractionation of Lignocellulosic Biomass to Produce Uncondensed Aldehyde-Stabilized Lignin. *Nat. Protoc.* **2019**, *14* (3), 921.

(31) Zhu, Y.; Liao, Y.; Lv, W.; Liu, J.; Song, X.; Chen, L.; Wang, C.; Sels, B. F.; Ma, L. Complementing Vanillin and Cellulose Production by Oxidation of Lignocellulose with Stirring Control. *ACS Sustainable Chem. Eng.* **2020**, *8* (6), 2361–2374.

(32) Schutyser, W.; Kruger, J. S.; Robinson, A. M.; Katahira, R.; Brandner, D. G.; Cleveland, N. S.; Mittal, A.; Peterson, D. J.; Meilan, R.; Román-Leshkov, Y.; Beckham, G. T. Revisiting Alkaline Aerobic Lignin Oxidation. *Green Chem.* **2018**, *20* (16), 3828–3844.

(33) Wu, X.; Fan, X.; Xie, S.; Lin, J.; Cheng, J.; Zhang, Q.; Chen, L.; Wang, Y. Solar Energy-Driven Lignin-First Approach to Full Utilization of Lignocellulosic Biomass under Mild Conditions. *Nat. Catal.* **2018**, *1* (10), 772–780.

(34) Mendu, V.; Shearin, T.; Campbell, J. E.; Stork, J.; Jae, J.; Crocker, M.; Huber, G.; DeBolt, S. Global Bioenergy Potential from High-Lignin Agricultural Residue. *Proc. Natl. Acad. Sci. U. S. A.* **2012**, *109* (10), 4014–4019.

(35) Li, W.; Amos, K.; Li, M.; Pu, Y.; DeBolt, S.; Ragauskas, A. J.; Shi, J. Fractionation and Characterization of Lignin Streams from Unique High-Lignin Content Endocarp Feedstocks. *Biotechnol. Biofuels* **2018**, *11* (1), na DOI: 10.1186/s13068-018-1305-7.

(36) Bunzel, M.; Schüßler, A.; Tchetsebu Saha, G. Chemical Characterization of Klason Lignin Preparations from Plant-Based Foods. *J. Agric. Food Chem.* **2011**, *59* (23), 12506–12513.

(37) Li, Y.; Shuai, L.; Kim, H.; Motagamwala, A. H.; Mobley, J. K.; Yue, F.; Tobimatsu, Y.; Havkin-Frenkel, D.; Chen, F.; Dixon, R. A.; Luterbacher, J. S.; Dumesic, J. A.; Ralph, J. An “Ideal Lignin” Facilitates Full Biomass Utilization. *Sci. Adv.* **2018**, *4* (9), 2968–2978.

(38) Mendu, V.; Harman-Ware, A. E.; Crocker, M.; Jae, J.; Stork, J.; Morton, S.; Placido, A.; Huber, G.; DeBolt, S. Identification and Thermochemical Analysis of High-Lignin Feedstocks for Biofuel and Biochemical Production. *Biotechnol. Biofuels* **2011**, *4* (1), na DOI: 10.1186/1754-6834-4-43.

(39) Ralph, J.; Lapierre, C.; Boerjan, W. Lignin Structure and Its Engineering. *Curr. Opin. Biotechnol.* **2019**, *56*, 240–249.

(40) Thornburg, N. E.; Pecha, M. B.; Brandner, D. G.; Reed, M. L.; Vermaas, J. V.; Michener, W. E.; Katahira, R.; Vinzant, T. B.; Foust, T. D.; Donohoe, B. S.; Román-Leshkov, Y.; Ciesielski, P. N.; Beckham, G. Mesoscale Reaction-Diffusion Phenomena Governing Lignin-First Biomass Fractionation. *ChemSusChem* **2020**, *13*, 4495.

(41) Kang, K.-Y.; Hwang, K.-R.; Park, J.-Y.; Lee, J.-P.; Kim, J.-S.; Lee, J.-S. Critical Point Drying: An Effective Drying Method for Direct Measurement of the Surface Area of a Pretreated Cellulosic Biomass. *Polymers* **2018**, *10* (6), 676.

(42) Anderson, E. M.; Stone, M. L.; Katahira, R.; Reed, M.; Muchero, W.; Ramirez, K. J.; Beckham, G. T.; Román-Leshkov, Y. Differences in S/G Ratio in Natural Poplar Variants Do Not Predict Catalytic Depolymerization Monomer Yields. *Nat. Commun.* **2019**, *10* (1), na DOI: 10.1038/s41467-019-09986-1.